NASA TECHNICAL MEMORANDUM

NASA TM X-71591

NASA TM X-71591

EFFECTS OF FORWARD VELOCITY AND ACOUSTIC TREATMENT ON INLET FAN NOISE

by Charles E. Feiler
Lewis Research Center
Cleveland, Ohio 44135

and

James E. Merriman
Douglas Aircraft Company
Long Beach, California 90846

TECHNICAL PAPER proposed for presentation at Sixth Aircraft Design Flight Test and Operations Meeting sponsored by the American Institute of Aeronautics and Astronautics
Los Angeles, California, August 12-14, 1974

EFFECTS OF FORWARD VELOCITY AND ACOUSTIC TREATMENT ON INLET FAN NOISE

by

Charles E. Feiler*
National Aeronautics and Space Administration
Lewis Research Center
Cleveland, Ohio

and

James E. Merriman+
Douglas Aircraft Company
Long Beach, California

E-8045

ABSTRACT

Flyover and static noise data from several engines are presented that show inlet fan noise measured in flight can be lower than that projected from static tests for some engines. The differences between flight and static measurements appear greatest when the fan fundamental tone due to rotor-stator interaction or to the rotor alone field is below cutoff. Data from engine and fan tests involving inlet treatment on the walls only are presented that show the attenuation from this treatment is substantially larger than expected from previous theories or flow duct experience. Data showing noise shielding effects due to the location of the engine on the airplane are also presented. These observations suggest that multiringed inlets may not be necessary to achieve the desired noise reduction in many applications.

INTRODUCTION

The route to low noise turbofan engines consists of increasing engine bypass ratio to reduce jet velocity and thus jet noise, applying low noise features to the fan stage design and incorporating acoustic treatment in the engine inlet and exhaust ducts. The success of these measures is demonstrated by the reduced noise levels of the wide-body aircraft whose engines employ these features. Further demonstration to even lower fan noise levels was achieved in the NASA Quiet Engine Program[1,2,3]; however, not without significant performance penalties due to the use of acoustically treated rings in the engine inlet and exhaust ducts.

---

*Head, Acoustics Section; Member AIAA

+Section Manager, External Acoustics Design; Member AIAA

Low noise fan stage design features that have been used are: deletion of inlet guide vanes; use of single stage fans; wide spacing between rotor and stator; and selection of rotor and stator blade numbers to provide cutoff of the fan fundamental tone due to rotor wake-stator interaction as described by Tyler and Sofrin[4]. These features are specifically predicated on rotor wake-stator interaction as the source of fan noise, as are several other ideas such as leaned stators and serrated leading edges on rotor blades. The benefit of these features is limited to operating tip speeds of the fan below that at which significant multiple pure tone or buzz-saw noise is encountered.

Static tests of fan stages with these features uniformly show the presence of the fan fundamental tone in far-field noise data even during operation at low subsonic tip speeds. The explanation for this observation currently receiving wide acceptance is that unsteady or distorted inflows exist in static testing and that these inflow disturbances interact with the rotor to produce sound in propagating modes[4,5,6,7,8]. Other experiments have shown a dramatic influence of the static test installation configuration on source noise where the effect was presumed to be due to inflow distortion and was analyzed as such[9].

The most significant effect, however, appears to be that observed during forward flight. Comparisons of ground static data with flight data for the RB211 engine[5] and the JT15D engine[10] show that the fan fundamental tone can be as much as 15 dB less in flight than in static testing. To confirm and further explore this flight effect, the first part of this paper presents and discusses data comparing flight noise with ground static noise obtained for the JT3D engine installed on a DC-8 aircraft and for the CF6 and JT9D engines installed on a DC-10 aircraft.

The effectiveness of acoustic treatment in reducing the noise radiation from engine inlet and exhaust ducts has been demonstrated in numerous experiments. For example, in one of the earlier programs, the Douglas Aircraft Company was able to demonstrate a noise reduction of 10.5 EPNdB at the FAR Part 36 approach condition for the DC-8 aircraft with nacelles consisting of a single splitter ring plus wall treatment in the inlet and a short treated fan exhaust duct[11]. In the same experimental program, The Boeing Company demonstrated a noise reduction of 15.5 EPNdB at the FAR Part 36 approach condition for the 707 aircraft with nacelles consisting of two splitter rings plus wall treatment in the inlet and a long treated fan exhaust duct (exit plane coplanar with the primary nozzle)[12]. In the

later NASA Quiet Engine Program, a noise reduction of about 9 EPNdB based on projections of static data was achieved for engine "A" with a nacelle consisting of a three-ring inlet and a single-ring exhaust duct[3]. In this latter program, the baseline engine was some 20 EPNdB quieter than the JT3D engine used in the previously mentioned programs. More recently, a 21 PNdB noise reduction was demonstrated statically in a STOL technology program on the TF-34 engine using a nacelle consisting of three inlet rings and two exhaust duct rings[13].

The foregoing illustrations give ample evidence of the ability of acoustic treatment to reduce engine component noise. The studies also revealed the associated appreciable performance losses that result from the extensive use of acoustic treatment, particularly from inlet splitter rings. These results point to the need for increased efficiency of the acoustic performance of treatment to retain the acoustic benefits but with smaller penalties. In particular, it is desired to reduce or eliminate the need for inlet splitter rings.

Data from several experiments are presented in the second part of this paper to show the performance of inlet suppressors without rings. The results are then discussed and interpreted with respect to duct propagation theories.

The final discussion deals with engine installation effects, particularly those related to the acoustic shielding of engine inlets by the airplane structure. Data are presented that show that shielding also can be a significant factor influencing inlet fan noise radiation and treatment requirements during approach.

EFFECTS OF FORWARD VELOCITY

The flight noise data presented were measured by the Douglas Aircraft Company. The measuring technique employed included a series of ground microphones and sophisticated techniques for tracking the aircraft flight path including the airplane position and speed relative to the observation point. Engine corrected speed was carefully controlled and atmospheric weather conditions were monitored. A more detailed discussion of the measurement procedures followed is found in reference 14.

The static noise data were measured on an engine test stand with far-field microphones located at 10° intervals on a 150-foot radius. In order to compare static data with flight data, it was necessary to project the static data to the flight conditions. The procedures used accounted for the number of engines, aircraft flight path, air speed and altitude, atmospheric absorption, Doppler shift and acoustic path length. Appropriate corrections were also applied to the jet noise component of the spectra to account for the effect of relative velocity on this noise component.

Comparisons of Flight and Static Noise Levels

The comparisons made in this section are at the FAR Part 36 approach measuring point with the aircraft engines at the appropriate approach thrust levels.

JT3D Engine. - Flight data for the JT3D engine were obtained on a DC-8 installation where the engine nacelles have fixed geometry inlets and no acoustic treatment. Figure 1 compares the tone corrected perceived noise level (PNLT) histories obtained from flight data with static data projected to the flight condition. The two sets of data were aligned along the time axis so that the times of maximum PNLT were matched. It can be seen that flight and projected static data agree to within 1 to 4 PNdB. A spectral comparison of inlet engine noise at an inlet angle of about 75°, about 1.5 seconds prior to the time of maximum PNLT, is shown in Figure 2. The comparison shows reasonable agreement between the two spectra, each having the same general spectral content and levels. Although not shown, similar spectral agreement was observed at the maximum PNLT values. The maximum PNLT values occurred after the aircraft passed overhead and they therefore are associated with aft-radiated engine and fan noise. For the JT3D engine, the data thus show that reasonable agreement exists between flight data and static noise prediction.

CF6 Engine. - Flight data on this engine were obtained on a DC-10 installation where the nacelles have fixed geometry inlets and acoustic treatment on the cowl walls. A comparison of flight and projected static PNLT time histories is shown in Figure 3. For this engine, the flight data are 3 to 12 PNdB less than the static projection depending on the time or position at which the comparison is made. Figure 4 shows a spectral comparison of these data at an inlet angle of about 70° corresponding to the peak inlet fan noise. While the static data clearly reveal the presence of the fan fundamental tone, it is absent in the flight data. At frequencies higher than the fan fundamental frequency, the projections from the static data remain higher than the flight data. A similar overprediction was observed for the JT3D flight-static comparison in Figure 2.

The trends of Figure 4 were also observed when the spectra were compared at the maximum PNLT values. The maximum values correspond to aft-radiated noise for this engine just as for the JT3D engine. Thus, for the CF6 engine, a major difference between flight and static data is the absence of the fan fundamental tone in the flight data. The absence of this tone probably accounts for a significant part of the reduction in flight PNLT values relative to the static projections.

JT9D Engine. - This engine was also flight tested on a DC-10 aircraft with fixed geometry inlets and acoustically treated cowl walls. Following the presentation sequence established, Figure 5 compares PNLT time histories for the flight and static projection cases. As in the case of the CF6 engine, the flight data are less than the static projection, in this case by 3 to 8 PNdB. The inlet noise spectral comparison,

shown in Figure 6 at an inlet angle of 60°, shows trends similar to those for the CF6 engine; however, for the JT9D engine, the flight data reveal the presence of the fan fundamental and second harmonic tones but at appreciably reduced levels compared to the static projection values. Trends similar to those in Figure 6 were observed at the maximum PNLT values which again correspond to aft-radiated noise. Thus, although fan tones were present in the flight spectra of the JT9D engine, they were at reduced levels compared to static spectra and the lower levels probably also account for much of the reduction in flight PNLT values.

The data presented thus far have been for an engine thrust or rpm setting and the corresponding aircraft weight conditions that would be used for a landing approach under FAR Part 36 conditions. For the JT9D engine, data were obtained at other engine rpm settings that, with the proper aircraft weight and trim conditions, could also be used for landing approach. Thus, Figure 7 shows the variations of PNLT with engine rpm for flight and static projection to flight for a JT9D-powered DC-10. The comparison is for inlet engine noise again at the FAR Part 36 approach measurement location. As can be seen, the flight values are less than the static projections at all values of engine rpm setting shown. The data also indicate that the difference decreases as engine rpm is increased. A similar behavior was observed for the RB211 engine as indicated by measurement of the fan fundamental tone[5]. For that engine, at fan blade tip Mach numbers somewhat greater than unity, the tone levels in flight and static data were nearly the same.

In the following section, possible interpretations and explanations for the behavior of these data (Figs. 1-7) will be discussed.

Fan Noise Theory

In order to interpret or explain the observed behavior of and differences between the flight and static noise data, it is appropriate to briefly review the noise sources and generation models that are usually considered for fan noise.

Noise Sources and Generation Models. - For the noise radiated forward of the engine, it is reasonable to consider that the source is inlet fan noise. Further, the differences between the flight data and the projected static data generally are at the fundamental fan tone and higher frequencies in the spectra, and the sources therefore are those that cause fan tones and broadband noise. At the approach engine condition for low relative tip Mach numbers, multiple pure tone or buzz-saw noise is not a significant source.

Figure 8 summarizes the sources of pure tone and broadband noise in an axial flow fan stage. Pure tones may arise from the rotor-alone field. They are also caused by stationary inflow distortions or large scale inlet turbulence interacting with the fan rotor or by the periodic component of rotor wakes interacting with the stators. Broadband noise is caused by small scale inlet turbulence or vortex shedding interacting with the rotor or by the random unsteady component of rotor wakes interacting with stators.

Two models have been developed to account for the sound generation. In the often discussed dipole model, the unsteady flows interact with the blades to produce unsteady lift forces resulting in dipole noise. In the quadrupole model, these same unsteady flows interact with the potential flow field around the blades to produce unsteady Reynolds stresses resulting in quadrupole noise[15].

Tyler-Sofrin Cutoff Theory. - An additional noise feature included in some fan stage designs is the selection of rotor and stator blade numbers such that the fundamental tone due to rotor-stator interaction does not propagate. The theory for this phenomena was developed in references 4 and 6. The criteria establishing whether the tones from this mechanism propagate or decay in a cylindrical hard-walled duct with uniform axial flow is given by the cutoff ratio ξ_m as

$$\xi_m = \frac{M_m}{M_m^* \sqrt{1 - M_x^2}} \tag{1}$$

where M_m is the tip Mach number of the spinning pattern, M_m^* is its cutoff Mach number, and M_x is the axial flow Mach number. This equation applies for a spinning mode of order m and the first radial mode. Propagation of the pattern occurs if the cutoff ratio ξ_m, is greater than unity and decay occurs if ξ_m is less than unity.

The tip Mach number of the pattern in terms of blade and vane number and rotor tip Mach number is given by

$$M_m = \frac{nBM_t}{nB + kV} \tag{2}$$

where n is the harmonic number, B and V are the numbers of rotor and stator blades respectively, M_t is the rotational tip Mach number of the rotor and k is an integer taking all positive and negative values. For $k = 0$, the equations describe cutoff for the rotor-alone sound field.

For a given rotational Mach number, M_t, these relations show that the cutoff ratio can be decreased by decreasing M_m which is accomplished by introducing a large number of stator vanes V relative to the number of rotor blades B. The use of the first radial mode in the criteria is conservative, since if the pattern involving the first radial mode is cutoff, all higher order radial modes are also cutoff. It has also been found that a constriction in the duct or the presence of soft walls will tend to decrease the cutoff ratio relative to the uniform hard walled duct value[16].

Interpretation of Flight/Static Noise Data

From the discussion of theory, it is necessary to establish whether the fan tones due to either rotor-alone or rotor-stator interaction were above or below the critical cutoff ratio of unity in the preceding engine tests. For the JT3D engine (Figs. 1 and 2) these tones from either source are well above cutoff even at approach power. Their presence in any spectrum, flight or static, could therefore be expected. As was shown in Figure 2, this was the case. The reasonable agreement observed between the flight data and the projection of static data to flight for the JT3D engine suggests that the controlling source mechanisms were the same in both flight and static testing. While the data do not directly reveal the mechanism, both rotor-alone and rotor-stator interaction are possible sources from theoretical considerations.

The CF6 and JT9D engine data (Figs. 3-6) require a different interpretation. Cutoff ratios of the first three fan harmonics for these engines are shown in Figure 9 as functions of fan rotor speed. The cutoff ratios were calculated assuming a hard-walled cylindrical duct with uniform axial Mach number. For the fan fundamental tones, the cutoff ratios plotted are due to the rotor-alone. Cutoff ratios for this tone due to rotor-stator interaction are less than the rotor-alone values for both engines at all rotor speeds. Thus for both engines, the rotor-alone is the most likely source of a fundamental fan tone. As Figure 9 also shows, the higher harmonics of the fan fundamental tone are well above cutoff for both engines. The source of these tones is rotor-stator interaction.

Data for the CF6 engine, Figures 3 and 4, were at a rotor speed of 2579 rpm. At this speed, Figure 9 shows that the fundamental tone is cutoff and therefore should not propagate. The flight data suggest that cutoff of this tone was realized since it did not appear in the flight spectrum. Its presence in the static data suggests that it had to be produced by a different noise source during static testing. The source, as has been suggested, is thought to be inflow distortion or atmospheric turbulence[5,6,7,8].

Data for the JT9D engine exhibited trends similar to the CF6 data. The JT9D, Figures 5 and 6, were for a rotor speed of 2666 rpm. Figure 9 shows the fundamental fan tone to be very near cutoff at this speed. Thus, the decreased level of the fundamental tone in the flight data could be due to the tone being cutoff since it is very close to the critical cutoff ratio of unity. As mentioned earlier, the effect of a constriction in the inlet tends to decrease the cutoff ratio. If this effect were included in the cutoff calculations, the tone should appear to be cutoff. As was mentioned earlier, the tone does not appear in flight data at lower rotor speeds and thus it appears that cutoff was also realized for this engine in flight. The presence of the tone in static test data is believed due to the same cause as for the CF6 static test data; namely, the presence of inflow distortions or atmospheric turbulence reacting with the rotor. In general, the flight/static behavior observed for the CF6 and JT9D engines was similar to that observed for the RB211 engine[5] and the JT15D engine[10].

The absence or reduced in-flight level of the fan fundamental tone at approach rotor speeds seems to indicate that in flight (1) the cutoff condition can be realized, and (2) inlet inflow conditions are sufficiently "clean" and free of disturbances that they do not present a significant noise source.

For the static data, an interpretation consistent with that for flight data, suggests that unsteady inflows exist. Sofrin, et al, recognized ground vortices and free stream atmospheric turbulence as candidate noise sources in their early work[6]. More recent studies point to atmospheric turbulence as the source[7,17,18]. The evidence seems to point to very elongated eddies, formed by drawing large-scale atmospheric turbulence into the inlet, that result in fan tone noise because of their large axial scale.

Aside from the disturbing conclusion that static fan or engine data are to some degree unreliable because of the presence of unsteady inflows, the important conclusion from flight data is that these unsteady inflows are minimized and that cutoff can be realized to yield noise levels substantially less in flight than would be expected from projection of the static data to flight.

PERFORMANCE OF ACOUSTICALLY TREATED INLETS

The effectiveness of acoustic treatment, as was discussed in the INTRODUCTION, has been demonstrated in many experimental programs. In the following sections, data showing the performance of acoustic treatment when it is used on the inlet cowl walls only, as well as on cowl walls and inlet splitter rings, will be presented and compared with suppressor theory.

Suppressor Performance With and Without Splitter Rings

The three-ring inlet described in reference 19 was tested with and without the rings in two experiments. The first experiments were performed with fan "C" of the NASA/GE Quiet Engine Program in the Lewis Full-Scale Fan Facility. The other experiments were performed with engine "A" of the same program by the General Electric Company. Data from these experiments are presented in some detail to illustrate the behavior of the different inlet configurations. In the final comparison of theory with experiment two other sets of data are included. One set was performed with the three ring inlet under discussion using a fan stage designated QF-3[20]. The other set was obtained for the JT8D engine for an inlet consisting of only a treated cowl wall and an inlet with treated cowl wall, extended bullet and two splitter rings[21].

Suppressor Configurations. - The inlet suppressor tests included a baseline configuration, a configuration involving inlet treatment only on the cowl walls, and finally the fully treated cowl wall plus three-ring configuration. Figure 10 shows sketches and some dimensions of the treated configurations used in the engine "A" tests. Detailed descriptions of the treated sections are given in references 1 and 19. Figure 10(a) shows the baseline configuration consisting of multiple degree of freedom (MDOF) "fan frame" treatment. Figure 10(b) shows the configuration involving the inlet walls, formed by adding a second short section (20 inches) of MDOF treatment and a larger section (58 inches) of single degree of freedom (SDOF) treatment. This larger section was the outer wall of the three ring inlet[19]. These sections were both designed to provide maximum attenuation, nominally, of the fan fundamental tone. The MDOF treatment should also provide some additional attenuation at higher frequencies in the range of the fan second harmonic tone. For this configuration a treated section including a splitter was added to the fan exhaust duct.

Figure 10(c) shows the addition of the three splitter rings in the inlet. As described in reference 19, the opposing walls of the passages formed by these splitter rings were designed to attenuate at two different frequencies such as the fan fundamental and second harmonic frequencies. This design feature thus provides a broader attenuation bandwidth. The lining designed for the higher of the two frequencies was on the outer or convex surfaces of the splitters while that for the lower was on the inner or concave surfaces of the splitters and on the cowl wall.

The configurations for the fan "C" experiments were similar to those just described for engine "A", except that all aft fan duct configurations, including the baseline, consisted of extended wall treatment and a splitter as shown in Figures 10(b) or (c). Also, the fan "C" inlet was 20 inches

shorter because the additional section of MDOF treatment shown in the inlet in Figures 10(b) or (c) was not used. While the configurations for engine "A" and fan "C" were not identical, they serve to show the important differences as the inlet configuration was changed.

Fan "C" Inlet Suppressor. - Figures 11(a) and (b) show the variation of perceived noise level with angle from the inlet axis at 90% and 60% of the fan "C" design speed, respectively. At an inlet angle of 50°, the peak forward angle for the baseline configuration, attenuations of about 6.5 to 7 PNdB were observed when the walls were made soft and further attenuations of 4.5 to 5 PNdB were observed when the rings were added. Since, as was discussed, the same aft suppression was used in each of these configurations, the levels for angles greater than 90° were all about equal.

Inlet sound pressure level spectra are shown in Figure 12 for these three configurations. Figure 12(a) shows sound pressure levels at 90% of fan design speed. At this speed, the fan is operating supersonically and the spectrum for the baseline configuration shows the significant presence of multiple pure tone or buzz-saw noise in the frequency range from 500 to 1600 Hz. In the frequency range up to about 1600 Hz, it can be seen that the soft wall configuration provided a large attenuation with little further contribution by the three rings. At frequencies greater than about 1600 Hz, the attenuation by the wall-only configuration diminished with increasing frequency, while the rings provided a significant contribution.

Figure 12(b) shows sound pressure levels at 60% of fan design speed. At this speed the fan is operating subsonically and the baseline spectrum is dominated by the fan fundamental tone and its harmonics. It can be seen that the wall-only treatment was very effective in attenuating the fan fundamental tone and broadband noise in the frequency range up to about 3150 Hz. The rings were effective at frequencies greater than 2000 Hz which includes the harmonics of the fan fundamental tone.

The data in Figure 12 show that the wall-only treatment was effective at the lower frequencies covering a range which includes multiple pure tones, the fan fundamental tone, and broadband noise. The effectiveness in this frequency range corresponds to the design frequency range of the treatment. The effectiveness of the rings in the higher frequency range, likewise corresponds to the higher frequency treatment designed into these surfaces.

Engine "A" Inlet Suppressor. - The variation of perceived noise level with angle from the inlet is shown in Figures 13(a) and (b) at 90% and 60% of the fan design speed, respectively. At the peak inlet angle of 50°, the soft wall configuration provided 7 to 8 PNdB of attenuation, while the rings provided a further attenuation of 1.5 to 2 PNdB. It will be recalled

from the sketches of Figure 10, that this inlet included an extra 20 inches of MDOF treatment on the cowl wall to give approximately 1/3 more treated length than the inlet for fan "C". When this extra length is accounted for, assuming the same effectiveness per unit length of treatment, these amounts of suppression compare closely with the results from fan "C".

Sound pressure level spectra for engine "A" at an inlet angle of 50° are shown in Figure 14(a) and (b) for 90% and 60% of the fan design speed, respectively. Since the fan in engine "A" was designed for a subsonic tip speed, the baseline spectra are dominated by the fan fundamental tone and its harmonics at all power settings. These spectra show the cowl wall treatment to be very effective throughout the frequency range. This behavior is perhaps partly accounted for by the additional length of MDOF treatment. The contribution of the rings, while less than for fan "C", occurred in the higher frequency range above 2000 Hz. As was observed in the data for fan "C", these data also show that the fan fundamental tone was very effectively attenuated by the cowl wall treatment.

Comparisons with Theory

The interpretation of the experimental suppressor behavior may be best accomplished from the vantage point of the available theory, which was the procedure followed earlier for the interpretation of forward flight effects on fan source noise.

Suppressor Theory. - The essential ingredients of the suppressor attenuation problem are outlined in Figure 15. For a prescribed duct geometry, flow field, duct termination and input wave, the wave equation for axial propagation is solved with an impedance boundary condition on the duct walls. A second practical part of the problem is to express the complex wall impedance in terms of the wall construction.

One of the earliest studies of wave propagation in a soft-walled rectangular duct was performed by Cremer[22]. In a later study, Rice determined the optimum wall impedance and the associated maximum possible attenuation rate for a plane sound pressure wave propagating in a soft-walled cylindrical duct of infinite length[23]. The plane pressure wave was closely approximated by combining the first ten axisymmetric radial duct modes. This work was later extended to the rectangular duct case for a plane wave input. Numerous other cases are now in the literature accounting for such effects as sheared flow, finite duct length, and employing other input wave descriptions such as the least attenuated mode that was studied by Cremer.

Figure 16 illustrates some results from reference 23. In this figure the maximum possible sound power attenuation calculated from the

theory is shown as a function of a frequency parameter, $f\alpha/c$, where f is the sound frequency, α is the duct cross-sectional dimension given by the diameter for a cylindrical duct and by duct height for a rectangular duct, and c is the speed of sound. Curves are shown for both the cylindrical and rectangular duct for a value of $L/\alpha = 1$. The rectangular duct theory has been used as an approximation for the annular passages formed by adding splitter rings to an inlet.

The significance of the curves is that at each value of the frequency parameter, the wall impedance is determined to yield the maximum possible sound attenuation from this theory. It can be seen that the primary difference between the rectangular and cylindrical duct curves is that the attenuation values for the rectangular duct are about half those for a cylindrical duct. Both curves show the same rapid decrease in attenuation as the frequency parameter is increased. It is this decrease coupled with large attenuation goals, that led to the use of splitter rings in inlets and also fan exhaust ducts. The effect, at a given frequency, is to reduce the duct cross-sectional dimension (α) which should result in increased attenuation for a given duct length. In the next section, theoretical results in the form of Figure 16 will be compared with experimental results.

Ring Performance. - Figure 17 compares experimental data for ringed inlets with rectangular duct theory. Theoretical curves are shown for a plane wave and for the least attenuated mode entering the duct. The plane wave curve is shown for a duct length to height ratio of four, since this was approximately the value for the data. The experimental attenuation values for the ringed inlet were corrected for that portion of the outer wall that was unopposed by the rings. The correction was determined with the assumption that the attenuation by the outer wall treatment varied linearly with length. The data are at the frequency where this corrected attenuation value peaked. This frequency was generally greater than that of the fan fundamental tone.

The resulting data points in Figure 17 are a factor of two or more below the plane wave theoretical curve. This result is not surprising because the theoretical curve was developed for a duct with the opposing walls treated for the same frequency and with the optimum wall impedance to yield the maximum possible attenuation for this propagation model. The experimental data, on the other hand, were for a duct with the opposing walls treated for two entirely different frequencies to yield a broader bandwidth attenuation.

In addition to this important reason, there are other reasons that could contribute to the experimental data falling below the theoretical curves. For example, the experimental data were determined using the length of the outer splitter and the height of the outer passage. This seems to be a reasonable approximation but it may be incorrect because the resulting value of L/H may be larger than the true effective value.

Another factor is that the wall impedance was probably different that the optimum value of the theory and any off-optimum value would reduce the theoretical attenuation.

It should also be pointed out that the theory is developed on a power spectral density basis. Thus, the use of third-octave data may impact the measured attenuation, not so much for the baseline configuration where fan tones may dominate a third-octave band, but in the suppressed configuration where this is not necessarily the case. The attenuation determined from third-octave data would thus be less than the more correct narrowband attenuations. It is also possible that the measured attenuation was limited by the presence of a noise floor due to another source. Two candidate sources are the noise generated by flow over the acoustic surfaces and aft-radiated fan and jet noise.

There are thus several factors that could explain why the experimental data fall below the ideal maximum possible attenuation described by theory. Experimental data obtained from flow ducts where the conditions of the theory are closely approximated are generally quite well-described by this theory.

Wall-only Performance. - Figure 18 compares experimental data with cylindrical duct theory for inlets with walls-only treated. Theoretical curves are shown for a plane wave and the least attenuated mode entering the duct. The plane wave curve is shown for a duct length-to-diameter ratio of one, since this was about the value for the data. The data shown are at the frequency of peak attenuation which was generally at the frequency of the fan fundamental tone. For the fan "C", 90% speed point, the peak attenuation occurred at 800 Hz and was for multiple pure tone or buzz-saw noise. In the case of engine "A" data, the extra 20 inches of MDOF treatment was considered as an additional length having the same effectiveness as the main section. The appearance of these data in relation to the total data seems to support this assumption.

As shown by Figure 18, the experimental attenuation was a factor of from four to eight times greater than the theory predicts. This result is in striking contrast to past estimates, based on similar theoretical results, that indicated astronomical length requirements for effective attenuation by cowl walls. It should be pointed out that the experimental attenuations may be less than they could be for the same reasons discussed for the ring inlet attenuations. In the present case, however, it seems certain that the lack of agreement between theory and experiment is due to the inappropriateness of the theory.

Spinning Mode Theory. - Consideration of the large differences between the measured acoustic performance of the wall and the widely used theoretical predictions leads one to consider spinning sound modes for the input wave rather than the radial or simple transverse modes normally used. The propagation of spinning waves in soft-walled ducts has been recognized in the literature, but no generalized results have been published to the authors' knowledge.

An analysis to yield optimum wall impedance and maximum attenuation rate for spinning modes propagating in a soft-walled cylindrical duct with zero flow has been performed concurrently and independently by E. W. Ritzi at the Douglas Aircraft Company and E. J. Rice at the NASA-Lewis Research Center. Figure 19 shows some of their unpublished results, in the form of Figure 18, with the spinning mode number m as a parameter. The calculations were for the first radial mode for each spinning mode. The lower curve for $m = 0$, is the least-attenuated-mode curve shown in Figure 18.

As Figure 19 shows, a very wide range of attenuations is possible depending on the spinning mode number. It can also be seen that spinning mode theory can indeed account for the levels of the experimental data. Unfortunately, just as the radial or transverse modes were not known for the earlier theory, the spinning mode description is also not known for application to this theory. In static testing with the presence of both rotor-stator interaction and rotor-inflow distortion noise sources, a large number of propagating spinning mode patterns could be generated. The magnitude of the attenuation by a given suppressor therefore could be different in flight testing because of the differing inflow conditions and the resulting changes in modal structure that do occur between the two situations. Thus, there remains a deficiency with regard to the input wave structure which appears to be of great importance. The important conclusion, however, is that treatment on the cowl wall only is considerably more effective than had been thought. Needless to say, this is an area that needs more investigation, because of the implications with regard to the elimination of splitter rings and their attendant performance loss.

EFFECT OF WING SHIELDING

On some aircraft, the engine inlets are located relative to the wing such that favorable shielding of noise from ground observers occurs. For example, a sketch of the engine-wing relations on a DC-9 aircraft with JT8D engines is shown in Figure 20. As shown by the figure, with the flaps down in the approach setting, the shielding area is significant and should provide some benefit. It should also be possible to locate the engine over-the-wing and obtain some shielding of either inlet or exhaust noise depending upon the location of the engine with respect to the wing.

Figure 21 shows an approach PNLT time history for the DC-9 as observed from flyover data. Also shown is a time history projected from static data. The data show the shielding effect that occurs at forward angles in the flyover. Figure 22 shows a comparison of the flight and projected static spectra at an inlet angle of 60°. It can be seen that both spectra have the same general shape but that the flight spectrum is

appreciably lower than the projected spectrum at the higher frequencies associated with inlet fan noise. For JT8D engines, as in the case of the JT3D engine, tones from the rotor alone or from IGV-rotor and rotor-stator interaction are well above cutoff and should propagate. Therefore, without the shielding effect of the wing, one would have expected these data to appear as those of Figure 2 for the DC-8 aircraft where no wing shielding occurred.

Experiments on engine-over-the-wing shielding have been performed at NASA-Lewis using a model wing with the baseline unsuppressed engine "C" of the Quiet Engine Program. Figure 23 shows the PNLT time history calculated from static tests for the approach flight condition. Data are shown with and without the wing present. The wing position relative to the engine inlet is shown by the insert sketch. It can be seen that the presence of the wing reduced the inlet noise at the observer by about 10 PNdB.

These data indicate the benefit to be derived from locating the engine where shielding of the inlet is possible. Shielding appears to be effective for inlet noise reduction and would not introduce the performance penalties associated with the application of inlet splitter rings.

CONCLUDING REMARKS

Three recent aspects of the inlet fan noise problem have been discussed in this paper: (1) the beneficial effect of forward velocity on inlet fan noise; (2) the better-than-anticipated performance of inlet treatment on the cowl walls; and (3) the beneficial effect of wing shielding on inlet radiated fan noise.

The forward velocity effect points to the need for further research into the nature of fan noise generation with regard to the differences between flight and static testing. It also appears that knowledge of the modal structure of the sound field under both static and flight conditions should be a research goal if acoustic treatment is as sensitive to modal structure as analysis indicates. This information is important for static evaluation of acoustic treatment but even more important for the flight case where the amount and the performance of the treatment is critical.

For design applications, the data presented suggest that, in a flight environment, the use of inlet splitter rings may not be necessary if only moderately high noise reduction is needed. While it appears that inlet fan noise can be alleviated without undue penalty, there remains the problem of engine aft radiated noise. Even though inlet noise can be suppressed, effective perceived noise levels will not be greatly impacted unless the aft radiated noise is also reduced.

REFERENCES

1. Kazin, S. B. and Paas, J. E., "NASA/GE Engine "A" Acoustic Test Results," CR-121175, 1973, NASA.

2. Kazin, S. B. and Paas, J. E., "NASA/GE Engine "C" Acoustic Test Results," CR-121176, 1974, NASA.

3. Ciepluch, C. C., Montegani, F. J., Benzakein, M. J., and Kazin, S. B., "Quiet Engine Test Results," Aircraft Engine Noise Reduction, SP-311, 1972, NASA, pp. 183-214.

4. Tyler, J. M. and Sofrin, T. G., "Axial Flow Compressor Noise Studies," Transactions of the SAE Vol. 70, 1962, pp. 309-332.

5. Cumpsty, N. A., and Lowrie, B. W., "The Cause of Tone Generation by Aero-engine Fans at High Subsonic Tip Speeds and the Effect of Forward Speed," Paper 73-Wa/GT-4, ASME Winter Annual Meeting, Detroit, Mich., 1973.

6. Sofrin, T. G. and McCann, J. C., "Pratt and Whitney Aircraft Experience in Compressor Noise Reduction," paper presented at the 72nd meeting of the Acoustical Society of America, Los Angeles, Calf., Nov., 1966.

7. Metzger, F. B., and Hanson, D. B., "Low Pressure Ratio Fan Noise Experiment and Theory," Paper 72-GT-40, ASME Gas Turbine and Fluids Engineering Conference and Products Show, San Francisco, Calif.,]972.

8. Mani, R., "Noise Due to Interaction of Inlet Turbulence with Isolated Stators and Rotors," Journal of Sound and Vibration, Vol. 17, No. 2, Jul. 1971, pp. 251-260.

9. Povinelli, F. P., Dittmar, J. H., and Woodward, R. P., "Effects of Installation Caused Flow Distortion on Noise from a Fan Designed for Turbofan Engines," TN D-7076,]972, NASA.

10. Plucinsky, J. C., "Quiet Aspects of the Pratt and Whitney Aircraft JT15 Turbofan" Paper 730289, SAE Business Aircraft Meeting, Wichita, Kan., 1973.

11. Marsh, A. H., "Flyover Noise Levels of DC-8-55 Airplanes with Acoustically Treated Nacelles," NASA Acoustically Treated Nacelle Program, SP-220, 1969, NASA, pp. 41-62.

12. Atvars, J., Mangiarotty, R. A., and Walker, D. S., "Acoustic Results of 707-320B Airplanes with Acoustically Treated Nacelles," NASA Acoustically Treated Nacelle Program, SP-220, 1969, NASA, pp. 95-108.

13. Jones, W. L., Heidelberg, L. J., and Goldman, R. G., "Highly Noise Suppressed Bypass 6 Engine for STOL Application," TMX-71448, 1973, NASA.

14. Zwieback, E. L. "Flyover Noise Testing of Commercial Jet Airplanes." Journal of Aircraft, Vol. 10, No. 9, Sept., 1973, pp. 538-545.

15. Goldstein, M. E., Dittmar, J. H., and Gelder, T. F., "Combined Quadrupole-dipole Model for Inlet Flow Distortion Noise from a Subsonic Fan," TN D-7676, 1974, NASA.

16. Hogge, H. D., and Ritzi, E. W., "Theoretical Studies of Sound Emission from Aircraft Ducts," Paper 73-1012, AIAA Aero-Acoustics Conference, Seattle, Wash., 1973.

17. Clark, L. T., "Sources of Unsteady Flow in Subsonic Aircraft Inlets," paper presented at the 87th meeting of the Acoustical Society of America, New York, N.Y., April 1974.

18. Hanson, D. B., "Spectrum of Rotor Noise Caused by Atmospheric Turbulence," paper presented at the 87th meeting of the Acoustical Society of America, New York, N.Y., April 1974.

19. Rice, E. J., Feiler, C. E., and Acker, L. W., "Acoustic and Aerodynamic Performance of a 6-Foot Diameter Fan for Turbofan Engines. Part III-Performance with Noise Suppressors," TN D-6178, 1971, NASA.

20. Dittmar, J. H., and Groeneweg, J. F.: "Effect of Treated Length on the Performance of Full-Scale Turbofan Inlet Noise Supressors." NASA TN (to be published).

21. Frasca, R. L., "Noise Reduction Programs for DC-8 and DC-9 Airplanes," paper presented at the 87th Meeting of the Acoustical Society of America, New York, New York, April 1974.

22. Cremer, V. L., "Theory of Sound Attenuation in a Rectangular Duct with an Absorbing Wall and the Resultant Maximum Coefficient. Acustica, Vol. 3, No. 2, 1953, pp. 249-263.

23. Rice, E. J., "Attenuation of Sound in Soft-Walled Circular Ducts," Aerodynamic Noise, H. S. Ribner, ed., Univ. of Toronto Press, Toronto, 1969, pp. 229-249.

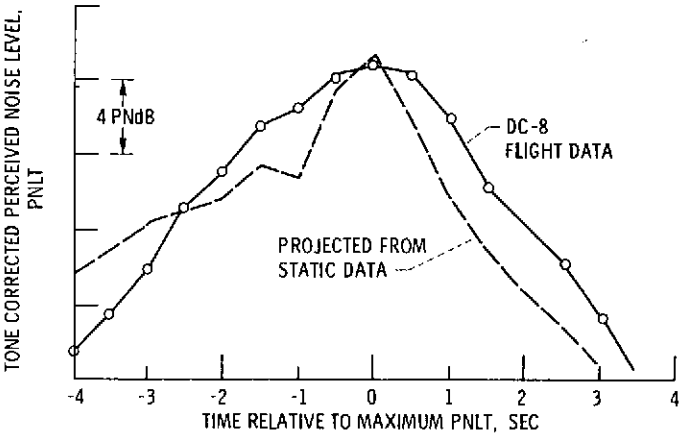

Figure 1. - Comparison of flight and projected static PNLT histories for JT3D-3B engine at approach condition (4696 rpm).

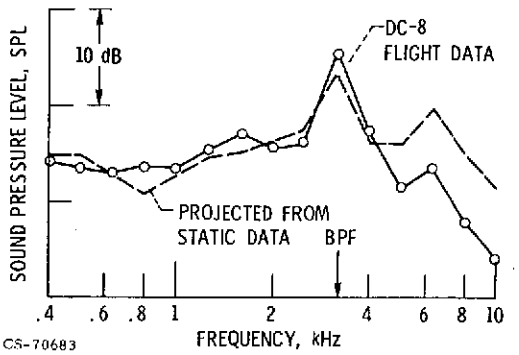

Figure 2. - Comparison of flight and projected static inlet sound pressure spectra for JT3D-3B engine at approach condition (4696 rpm); 75^0 inlet angle.

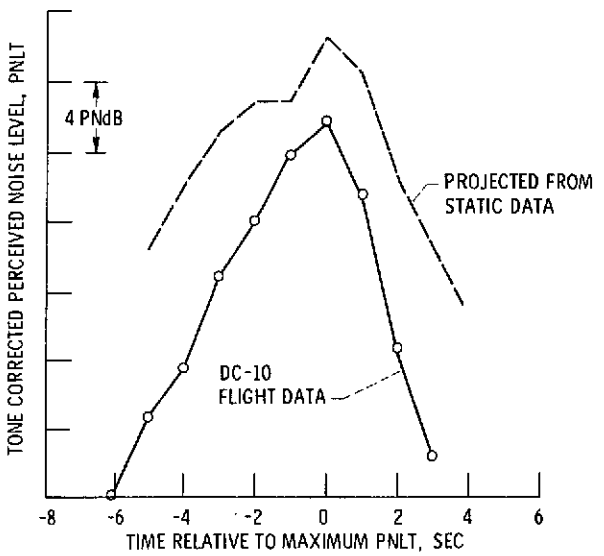

Figure 3. - Comparison of flight and projected static PNLT histories for CF6-6 engine at approach condition (2579 rpm).

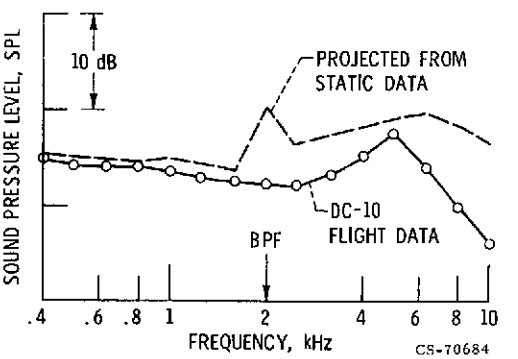

Figure 4. - Comparison of flight and projected static inlet sound pressure spectra for CF6-6 engine at approach condition (2579 rpm); 70^0 inlet angle.

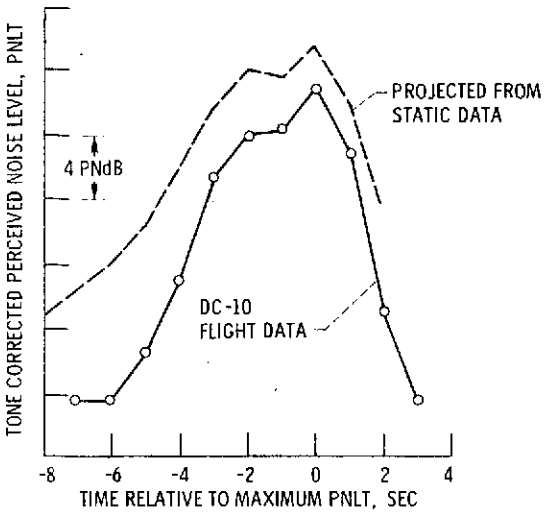

Figure 5. - Comparison of flight and projected static PNLT histories for JT9D-20 engine at approach condition (2666 rpm).

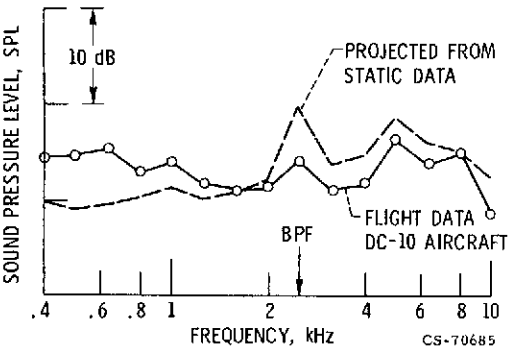

Figure 6. - Comparison of flight and projected static inlet sound pressure spectra for JT9D-20 engine at approach condition (2666 rpm); 60^0 inlet angle.

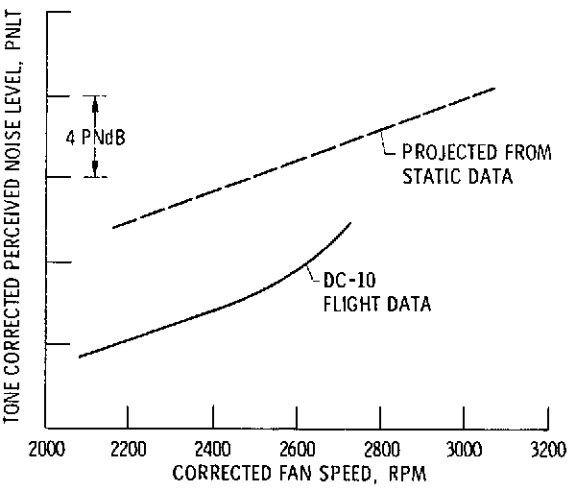

Figure 7. - Comparison of flight and projected static tone corrected perceived noise levels for inlet noise from a JT9D-powered DC-10 at part 36 approach condition. 60^0 inlet angle.

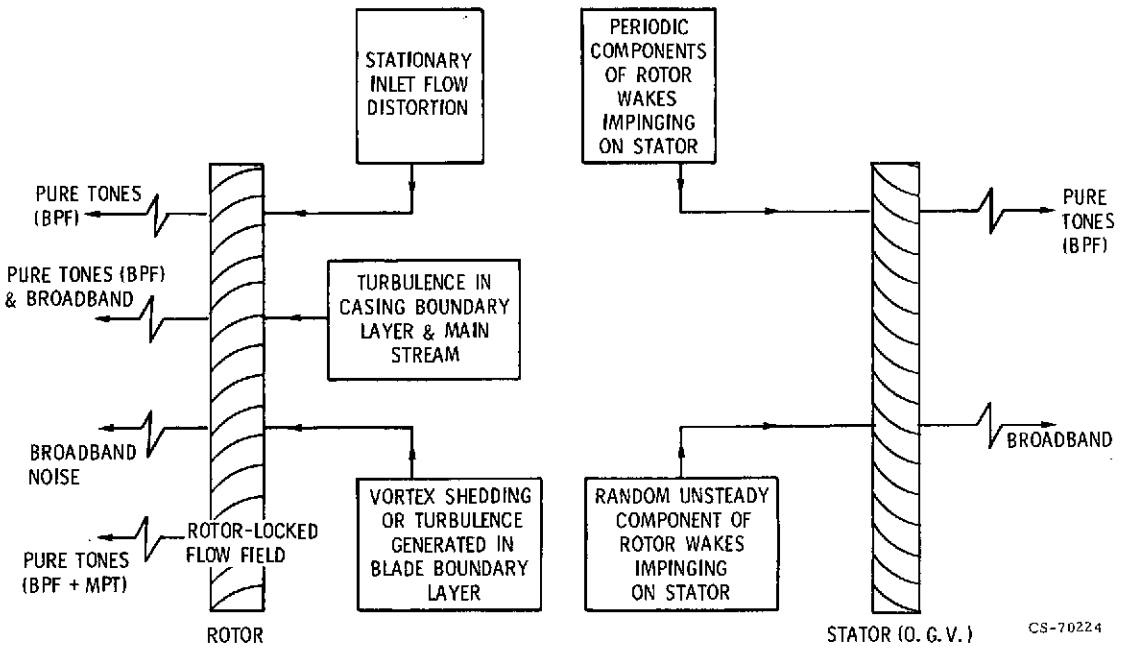

Figure 8. - Principal noise sources in axial flow fans.

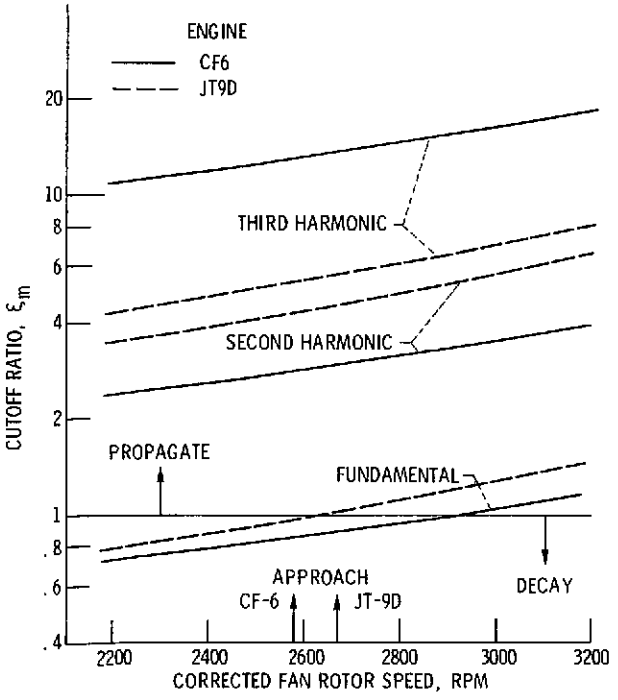

Figure 9. - Variation of cutoff ratio of fan tones with rotor speed.

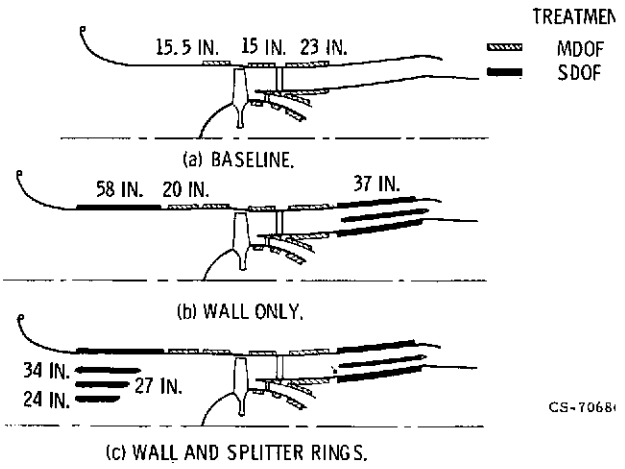

Figure 10. - Suppressor configurations for engine A tests.

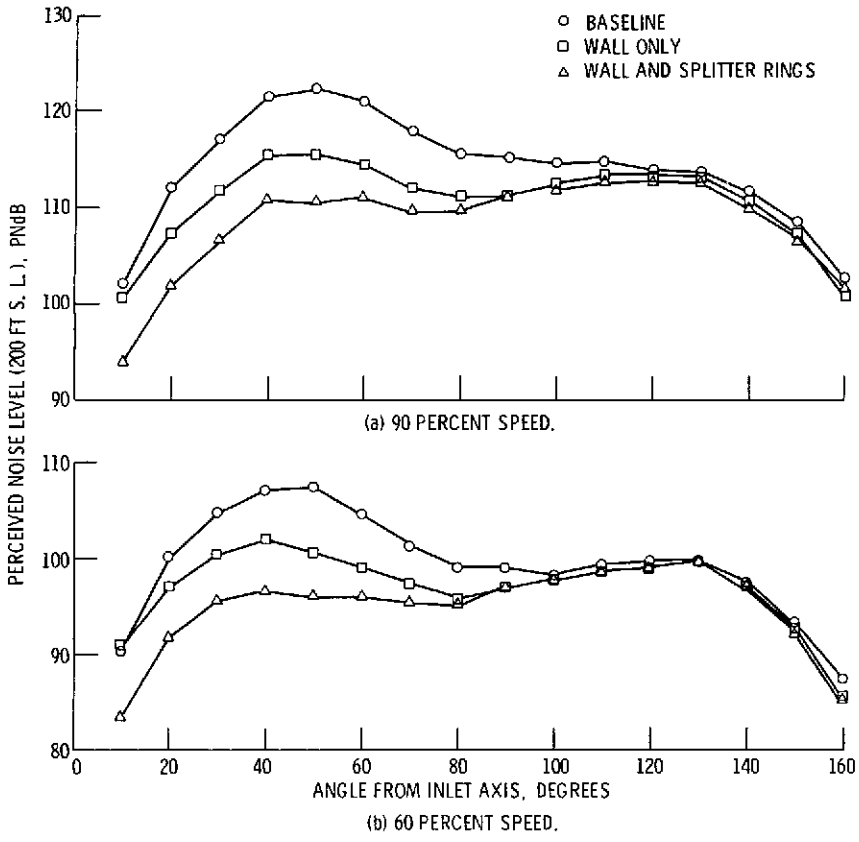

Figure 11. - Effect of inlet suppressor configuration on perceived noise level of fan C.

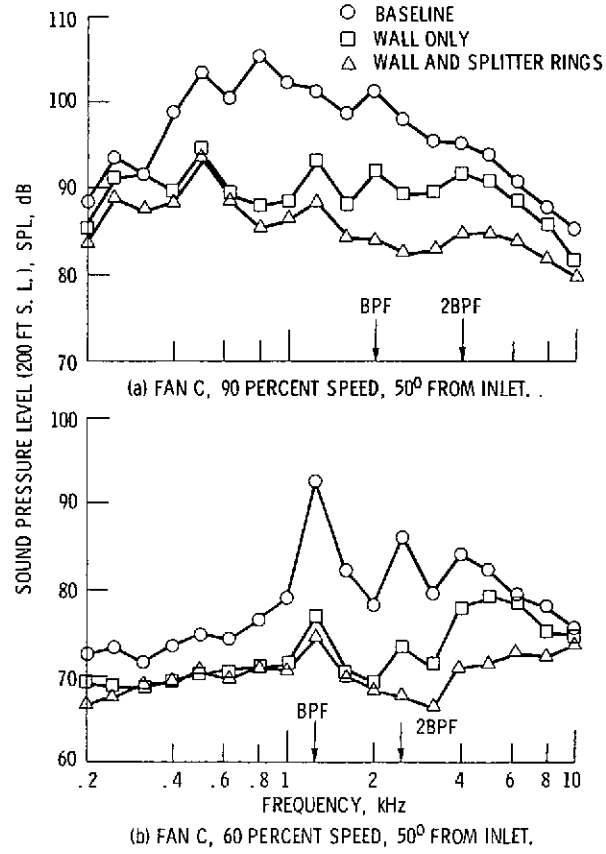

Figure 12. - Effect of inlet suppressor configuration on inlet sound pressure.

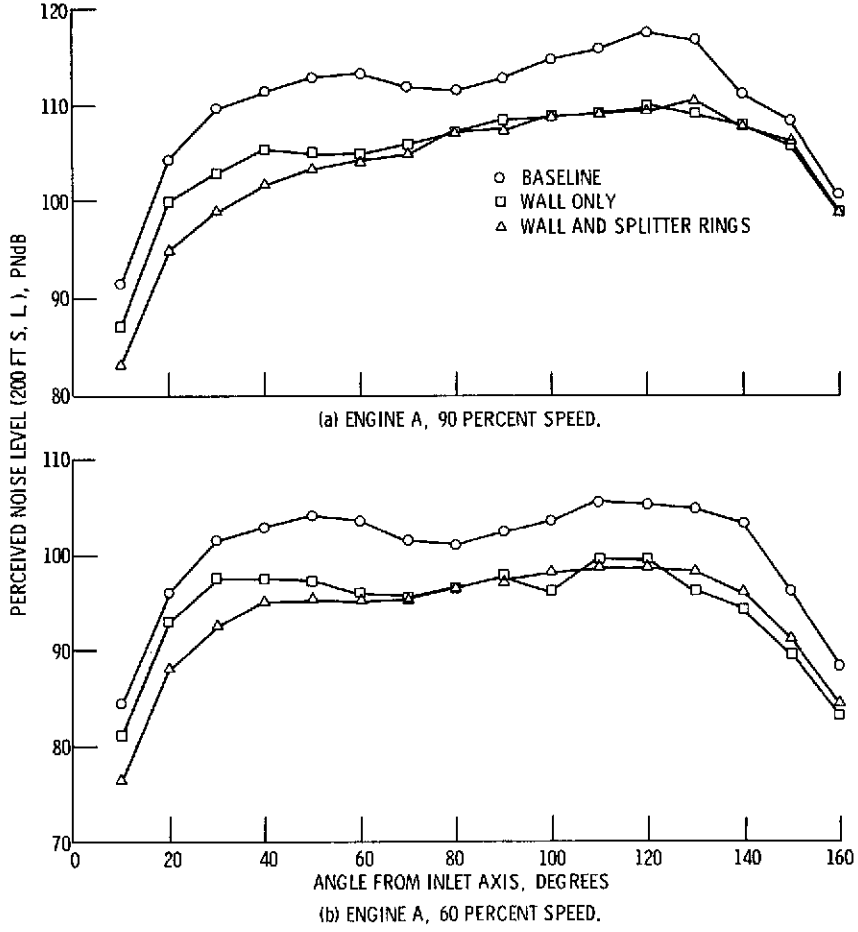

Figure 13. - Effect of inlet suppressor configuration on perceived noise level.

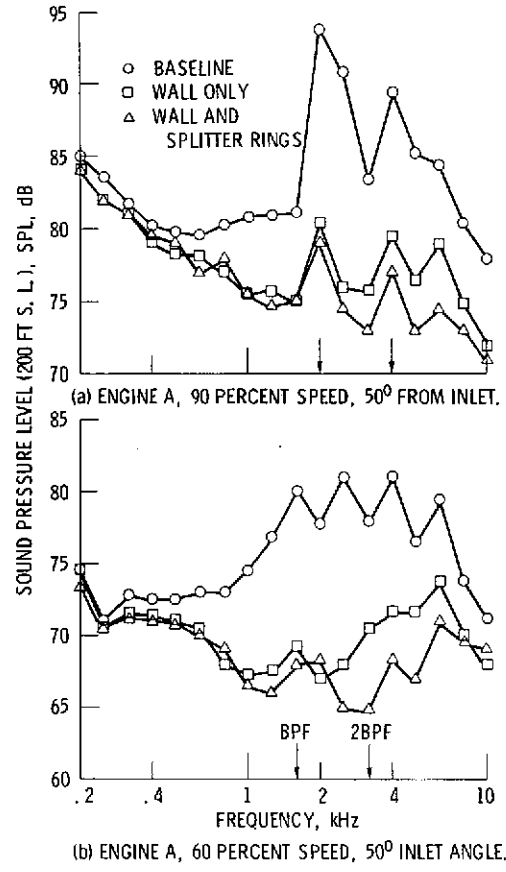

Figure 14. - Effect of inlet suppressor configuration on SPL spectrum.

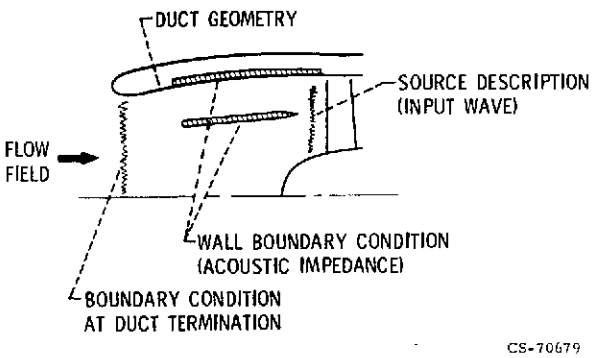

Figure 15. - Components of suppressor analysis.

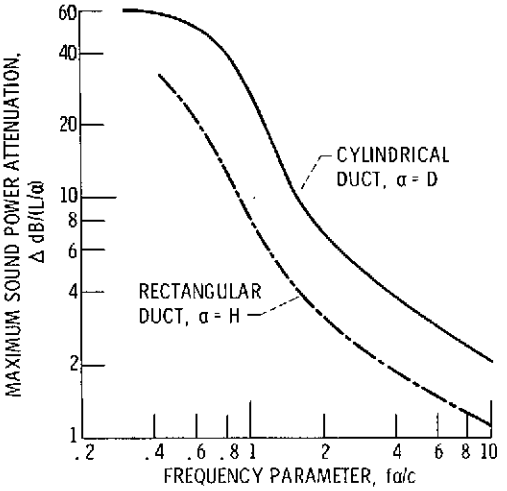

Figure 16. - Theoretical attenuation curves for plane pressure wave source, zero flow; L/α = 1.

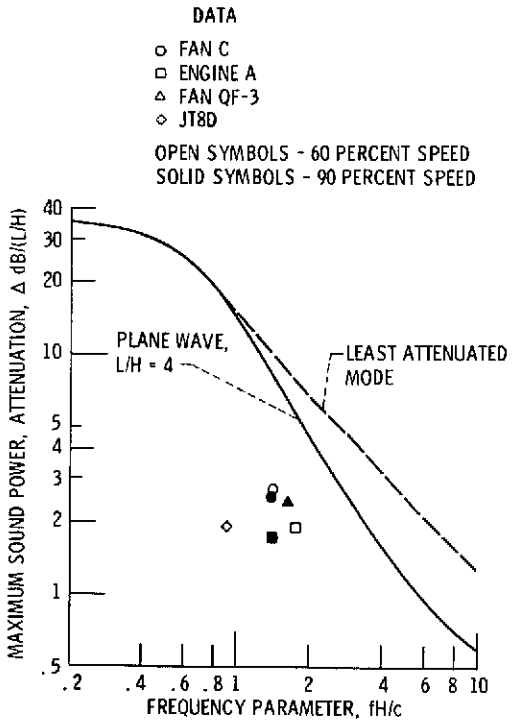

Figure 17. - Comparison of splitter ring performance with theory for no mean flow.

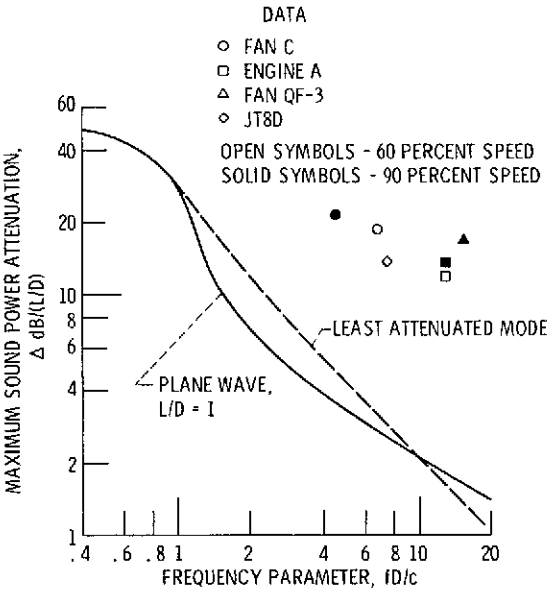

Figure 18. - Comparison of wall only performance with theory for no mean flow.

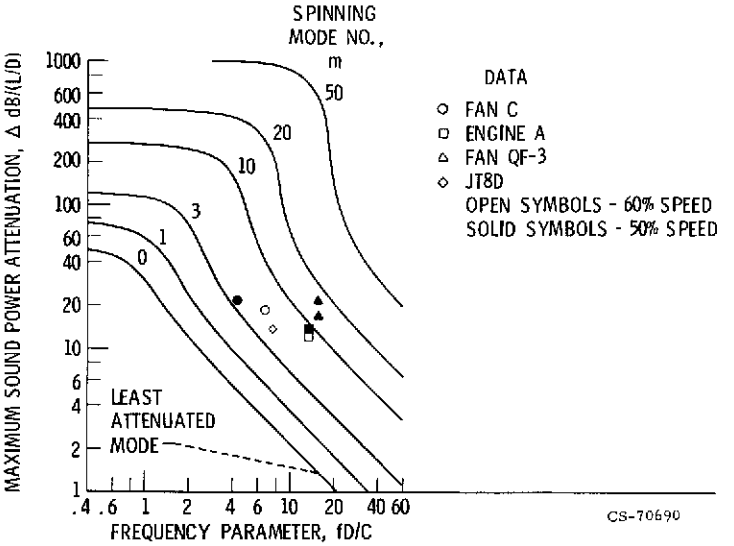

Figure 19. - Effect of spinning mode number on theoretical maximum sound attenuation in soft walled circular duct with no mean flow.

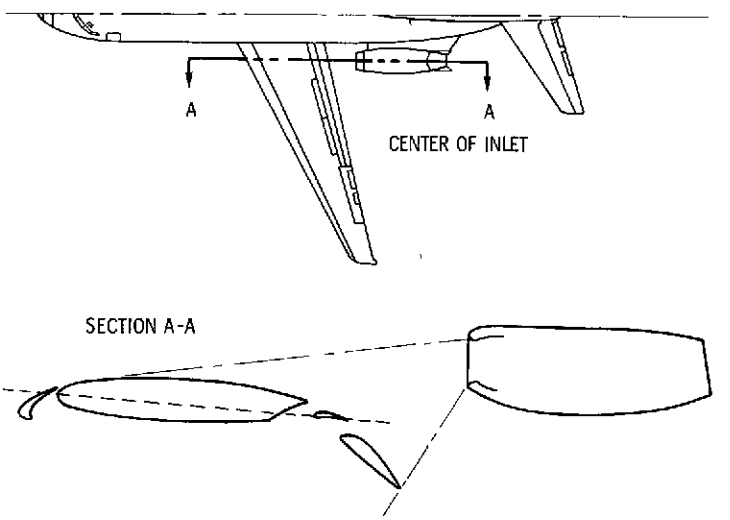

Figure 20. - DC-9 wing/nacelle spacing for 50° flaps.

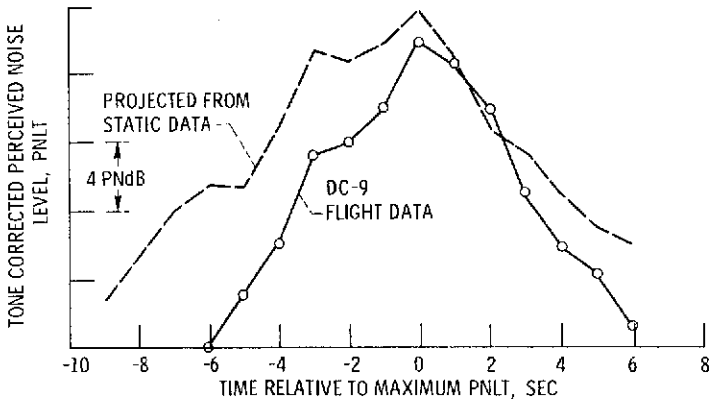

Figure 21. - Comparison of flight and projected static PNLT histories for JT8D-9 engine on DC-9 aircraft at approach condition (6159 rpm).

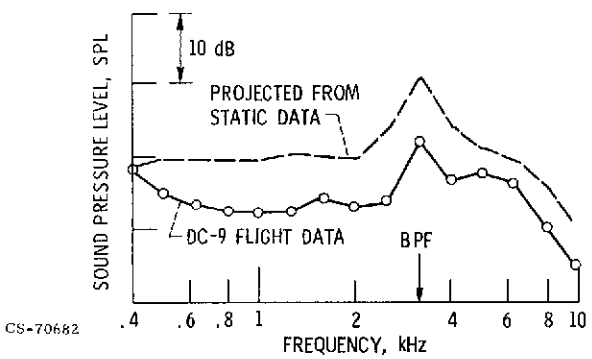

Figure 22. - Comparison of flight and projected static inlet sound pressure spectra for JT8D-9 engine on DC-9 aircraft at approach condition (6159 rpm); 60^0 inlet angle.

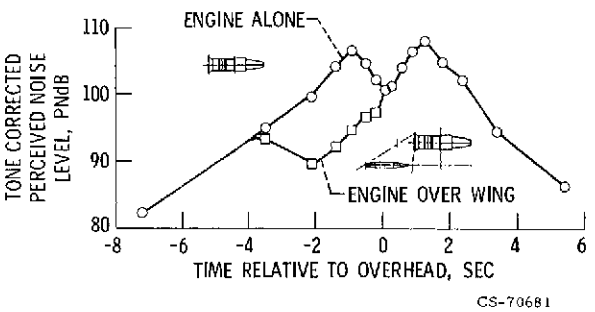

Figure 23. - Effect of wing shielding on PNLT history for engine C at approach condition.